Digital Control of a Single-Phase UPS Inverter for Robust AC-Voltage Tracking

Young-Tae Woo and Young-Chol Kim*

Abstract: This paper presents a digital controller for a single phase UPS inverter under two main considerations: (i) the overall system shall keep very low AC-voltage tracking error as well as no phase delay over different load conditions, and (ii) the digital controller shall be employed at a fixed sampling time. We propose that the former can be achieved by the proposed controller using the error-state approach and the latter can be dealt with by the so-called characteristic ratio assignment.

1. INTRODUCTION

In all UPS inverters, the goal is to maintain the desired output waveform with fast response and low total harmonic distortion (THD) over all loading conditions. This means that the UPS controller should work to properly maintain the sinusoidal waveform of output voltage even when the load changes abruptly. Basically, the THD is controlled by a L-C filter. In addition to this low pass filter, a feedback controller with good tracking performance can cause the THD to be further reduced.

The inverter systems with feedback controller are generally constructed in the form of either state feedback or double-loop feedback. The latter consists of a current-feedback loop as an inner loop and a voltage-feedback loop as an outer loop. Each loop has its own compensator. One of the most difficult problems associated with this control structure arises from the fact that the two loops are closely interconnected. Another problem may occur with a fixed sampling time when a digital controller is used.

It is well known that for a digital controller determined by the emulation method, a low sampling rate has been a constraint. As a result, one cannot make the speed of response faster than a certain value.

Young-Tae Woo is with Dept. of Electronics, Chungbuk National University, 48 Gaesin-dong, Cheong-ju, Chungbuk 361-763, Korea (e-mail: wytnice@chungbuk.ac.kr).

Young-Chol Kim is with the School of Elec. & Computer Eng., Chungbuk National University, 48 Gaesin-dong, Cheong-ju, Chungbuk 361-763, Korea (e-mail: yckim@cbu.ac.kr).
* Corresponding author.

In many cases, the digital controller for a UPS inverter must be designed under a given specified sampling time because of cost constraints. Also, the sampling time is limited by the switching frequency of the PWM inverter. Digital controllers incorporating various forms of state feedback have been developed [1-3].

In this paper, a digital controller for a single phase UPS inverter using the error-space approach is presented. The specifications to be satisfied are a THD less than 5%, a small overshoot in response to an abrupt load change (e.g., the case of a full load applied from a no load state at the peak phase of output voltage), and a fast step response. The performance of the resulting system is evaluated under the following three load conditions: no load, a resistive load of 10kW, and a nonlinear rectifier load of 10kW.

We first design a continuous-time controller for a continuous-time plant and then make the discretization of the controller with the given sampling time of 8kHz. The disadvantage of this method is that its fidelity depends on the sampling rate and on the discretization method. But it has a big advantage in that one can apply sufficient design methods developed for continuous-time linear systems. In this paper, we will employ the error-state feedback control scheme to carry out the robust AC-voltage tracking. The error-space approach [5] is an analytic state-feedback method to give a controller the ability to perfectly track a non-decaying input and to reject a non-decaying disturbance such as a sinusoidal input. Since this method solves the control problem in an error space, we are assured that the error approaches zero even if some parameters change. As shown in Section 3, the structure of this controller includes the internal model in the outer loop and the state feedback controller in the inner loop. However, when the configuration is transformed into a digital controller,

we are faced with the problem that the controller to be designed must meet not only the stability of the overall system but also that the response speed of the inner loop must be slower by at least 5~10 times that of the fixed sampling time. We will suggest a method to deal with this problem.

On the other hand, we introduce the characteristic ratio assignment (CRA) to achieve the time response requirements. It has been shown in [4-5] that the CRA has the ability to deal directly with the overshoot and speed of step response of an all-pole system of arbitrary order. The method is based on certain relationships between characteristic polynomial coefficients and transient responses. The CRA design formulates a model matching problem whose reference model is selected from a target polynomial. In our approach, the state feedback gains are determined by the CRA instead of the pole-placement method. Finally, the proposed method is evaluated using simulation results generated by Sim-power System Toolbox 3.0 from Simulink®.

2. UPS INVERTER MODEL AND PRELIMINARIES OF CRA

In this section, we describe the state-space model of a UPS inverter. Also some basic preliminaries of the CRA are given.

2.1. A UPS inverter model

Fig. 1 shows the simple configuration of a UPS inverter. In order to develop the model of this plant, we consider the following state variables: the capacitor current, i_c, and the capacitor voltage, v_c. The variables V_{dc}, i_d, i_o, V_a and Q_i denote DC-link voltage and current, inductor current, inverter output voltage, and IGBT switching elements, respectively. Then we have the following state-space model:

$$\dot{x}_1 = -\frac{R_f}{L_f}x_1 - \frac{1}{L_f}x_2 + \frac{1}{L_f}v_a - (i_o' + \frac{R_f}{L_f}i_o), \quad (1)$$

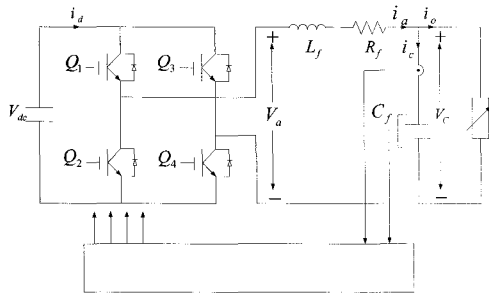$$\dot{x}_2 = \frac{1}{C_f}x_1, \quad (2)$$

$$y = v_c, \quad (3)$$

Fig. 1. UPS inverter system.

where $x_1 = i_c$, $x_2 = v_c$.

Rewriting (1) ~ (3) in vector form, the plant model becomes

$$\dot{x} = \begin{bmatrix} -\dfrac{R_f}{L_f} & -\dfrac{1}{L_f} \\ \dfrac{1}{C_f} & 0 \end{bmatrix} x + \begin{bmatrix} \dfrac{1}{L_f} \\ 0 \end{bmatrix} v_a - \begin{bmatrix} 1 \\ 0 \end{bmatrix} (i_o' + \dfrac{R_f}{L_f}i_o) \quad (4)$$

$$= Fx + Gu + G_1 w,$$

$$y = Hx = \begin{bmatrix} 0 & 1 \end{bmatrix} x, \quad (5)$$

where $x^T = \begin{bmatrix} x_1 & x_2 \end{bmatrix}$, $u = v_a$, $w = i_o' + \dfrac{R_f}{L_f}i_o$.

2.2. Preliminaries of CRA

Consider a linear system whose transfer function is

$$G(s) = \frac{n(s)}{p(s)} = \frac{b_m s^m + b_{m-1} s^{m-1} + \cdots b_0}{a_n s^n + a_{n-1} s^{n-1} + \cdots + a_0}. \quad (6)$$

The characteristic ratios are defined as

$$\alpha_1 = \frac{a_1^2}{a_0 a_2}, \quad \alpha_2 = \frac{a_2^2}{a_1 a_3}, \quad \cdots, \quad \alpha_{n-1} = \frac{a_{n-1}^2}{a_{n-2} a_n} \quad (7)$$

and the generalized time constant is defined to be

$$\tau := \frac{a_1}{a_0}. \quad (8)$$

Conversely, the coefficients a_i of $\delta(s)$ can be represented in terms of α_i's and τ as follows: for any a_0,

$$a_1 = a_0 \tau, \quad (9)$$

$$a_i = \frac{a_0 \tau^i}{\alpha_{i-1} \alpha_{i-2}^2 \alpha_{i-3}^3 \cdots \alpha_2^{i-2} \alpha_1^{i-1}}, \quad \text{for } i = 2, \cdots, n. \quad (10)$$

Let us define a polynomial whose coefficients are generated by using (9), (10) with arbitrarily chosen positive parameters a_0, τ and the characteristic ratios α_k's obeying the following formula:

(i) $\alpha_1 > 2$, $\quad (11)$

(ii) $\alpha_k = \dfrac{\sin(k\pi/n) + \sin(\pi/n)}{2\sin(k\pi/n)} \cdot \alpha_1 = \Gamma_k \cdot \alpha_1$,

for $k = 2, \cdots, n-1$. $\quad (12)$

We call this polynomial as the K-polynomial here. It is important to note that the K-polynomial is generated by only α_1 for a given τ and a_0. It is easy to see

that (12) holds the following relations.

(i) $\alpha_k = \alpha_{n-k}$, for $k = 1,2,\cdots,(m-1)$,

(ii) $\alpha_k > \alpha_{k+1}$, for $k = 1,2,\cdots,(m-2)$,

where $n = 2m$ even and $n = 2m-1$ odd.

Now we give a brief summary about what relationship between (α_k, τ) and time response is. The time constant is an important parameter since it determines the speed of the response. Although the definition of time constant is clear for the case of 1st order systems, the precise definition is not known when multiple time constants are present. Due to this unknown relationship between multiple time constants and the time response, it is difficult to achieve a desired speed of response when higher order transfer functions are involved.

The following Theorem 1 states that the speed of the response of a linear all pole system can be controlled, while maintaining the exact shape of the response, by adjusting the value of τ (or ratio of the two lowest order coefficients of the denominator polynomial) if its characteristic ratios can be kept the same. We call this τ the *generalized time constant*.

Theorem 1[4]: Consider two all pole transfer functions of the same degree $H_1(s)$, $H_2(s)$, of which the generalized time constants are τ_1 and τ_2, respectively. Let $y_i(t)$ be the step response of $H_i(s)$. Then

$$y_i(t) = y_2(\frac{\tau_1}{\tau_2} \cdot t) \tag{13}$$

if and only if both $H_1(s)$ and $H_2(s)$ share the same characteristic ratios.

For a given all pole system with its generalized time constant, the above can be used to determine a new generalized time constant that provides the desired speed of the response while maintaining the exact shape of the response. This property holds on the case of general transfer function having numerator polynomial.

Although the analytical relationships between damping and characteristic ratio are not yet known, the dependency can be explained by using the Kessler's multiple loop structure [8]. For the purpose of this discussion, let us consider the 2-loop system shown in Fig. 2.
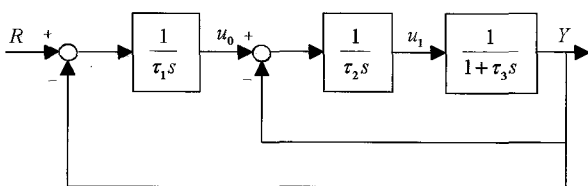

Fig. 2. Kessler's 2 loop structure.

The transfer function of the overall system is

$$T(s) = \frac{1}{1 + \tau_1 s[1 + \tau_2 s(1 + \tau_3 s)]}$$

$$= \frac{1}{\tau_1 \tau_2 \tau_3 s^3 + \tau_1 \tau_2 s^2 + \tau_1 s + 1}. \tag{14}$$

According to (7), the characteristic ratios of $T(s)$ are

$$\alpha_1 = \frac{\tau_1}{\tau_2}, \quad \alpha_2 = \frac{\tau_2}{\tau_3}. \tag{15}$$

Now, we consider the dynamics of the inner loop system. Its transfer function and the characteristic ratio are as follows:

$$T_i(s) = \frac{1}{1 + \tau_2 s(1 + \tau_3 s)} = \frac{1}{\tau_2 \tau_3 s^2 + \tau_2 s + 1},$$

$$\bar{\alpha}_2 = \frac{\tau_2}{\tau_3} = \alpha_2. \tag{16}$$

Secondly, if we assume that with $\tau_1 > \tau_2 > \tau_3$, $T(s)$ can be approximated as follows:

$$T(s) \approx \frac{1}{1 + \tau_1 s(1 + \tau_2 s)} = \frac{1}{\tau_1 \tau_2 s^2 + \tau_1 s + 1} := T_0(s),$$

then the characteristic ratio of $T_0(s)$ becomes

$$\bar{\alpha}_1 = \frac{\tau_1}{\tau_2} = \alpha_1. \tag{17}$$

Furthermore, it is easily seen that the damping ratio of a second-order system is identical to $\zeta = \frac{\sqrt{\alpha_1}}{2}$. Since the all-pole system of arbitrary order is also developed in the same manner, we can say from (16) and (17) that the characteristic ratio of an all-pole system is closely related to the damping.

The K-polynomial has very interesting properties. To begin with, recall that for fixed a_0 and τ, the polynomial can be composed by only a characteristic ratio α_1. In [4], they have showed that the all pole system $H_K(s)$ whose denominator is the K-polynomial guarantees the stability and that its frequency magnitude function is monotonically decreasing. Furthermore, we represent that the α_1 can be a single parameter that allows to adjust the damping of a polynomial. It shows that the damping of K-polynomial shall be increased as α_1 increases. In other words, if we make an all pole transfer function using K-polynomial, the system gives rise to smaller overshoot as α_1 increases. Fig. 3 shows that the

maximum overshoots of $H_K(s)$ with $n = 3,4,\cdots,8$ monotonically decrease with respect to α_1. Fig. 4 shows the root locus of a K-polynomial with respect
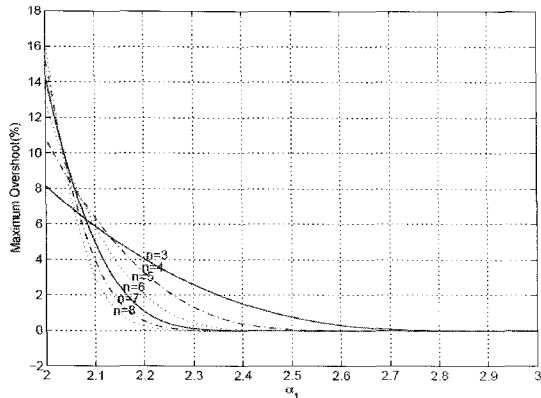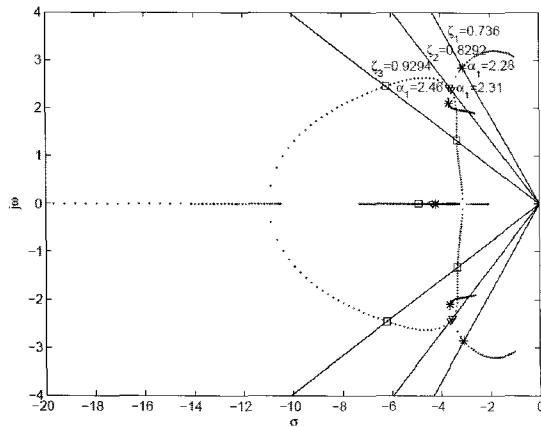

Fig. 3. Overshoots of $H_K(s)$ w.r.t. α_1.

Fig. 4. Root locus of a K-polynomial w.r.t. α_1.

Table 1. α_k's and poles of $H_K(s)$ resulting in non-overshoot (where $\tau = 1$).

n	$\alpha = [\alpha_1 \quad \alpha_2 \quad \cdots \quad \alpha_{n-1}]$	Roots
3	[2.836 2.836]	$-2.836,$ $-2.604 \pm 1.124i$
4	[2.646 2.259 2.656]	$-4.984 \pm 1.456i,$ $-2.924 \pm 0.854i$
5	[2.538 2.053 2.053 2.538]	$-7.686 \pm 2.137i$ $-5.209,$ $-3.277 \pm 0.911i$
6	[2.464 1.943 1.848 1.943 2.464]	$-11.01 \pm 2.89i,$ $-7.522, -5.633,$ $3.602 \pm 0.945i$
7	[2.411 1.874 1.742 1.742 1.874 2.411]	$-14.9 \pm 3.72i,$ $-10.53, -7.87,$ $-5.88, -3.91 \pm 0.98i$
8	[2.37 1.83 1.68 1.64 1.68 1.83 2.37]	$-19.35 \pm 4.62i,$ $-14.02, -10.8,$ $-7.97, -6.14,$ $-4.21 \pm 1.005i$

to α_1. Using this property of K-polynomial, it is very useful to obtain the all pole system of which step response has no overshoot.

In Table 1, the α_k of various $H_K(s)$ to have non-overshooting step response are given. The pole locations corresponding to the α_k are also included in the Table 1.

3. DESIGN OF A DIGITAL CONTROLLER FOR ROBUST AC-VOLTAGE TRACKING

Suppose that we want to design a controller for the UPS plant described in (4) and (5) so that the closed-loop system will have a good time response that is as fast as possible, while the controller has the ability to track a sine-wave command and reject non-decaying disturbances. For this purpose, the error-space approach is used. Fig. 5 shows a control structure of which the details are presented later in (33)~(35).

The controller consists of two parts. The first part (see box A in Fig. 5) is the state-feedback controller which mainly controls the current loop. We will take the time response requirement and limitation due to sample time into consideration when the feedback gain K_0 is determined.

The details of box A are shown in Fig. 6. The second part (box B in Fig. 5) plays a role in eliminating the tracking error. This is sometimes called the "Internal Model Principle." We first formulate the mathematical relations of the error-space model. Since the reference signal v_c^* is sinusoidal of frequency $\omega_0[rad / \sec]$, it follows that
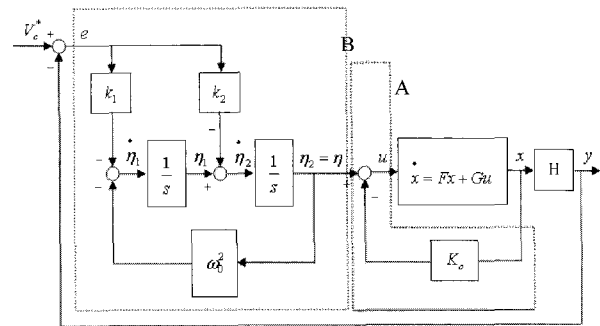

Fig. 5. Block diagram of the designed controller.
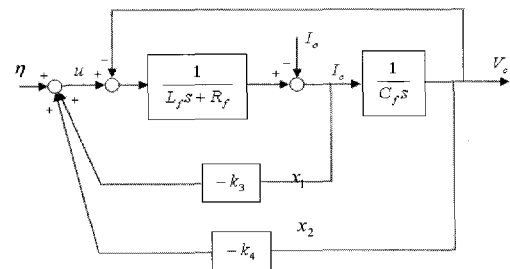

Fig. 6. Detailed diagram of box A.

$$\ddot{v}_c^* + \omega_0^2 v_c^* = 0 .$$ (18)

The tracking error is defined as

$$e := v_c^* - v_c = v_c^* - y .$$ (19)

Then we can write the error in terms of the state

$$\ddot{e} + \omega_0^2 e = -\left[H\ddot{x} + \omega_0^2 Hx \right].$$ (20)

Here, a new state vector and the control input in error space are defined as follows:

$$\xi := \ddot{x} + \omega_o^2 x ,$$ (21)

$$\mu := \ddot{u} + \omega_o^2 u .$$ (22)

With these definitions, it is easy to derive the relations

$$\dot{\xi} = F\xi + G\mu ,$$ (23)

$$\ddot{e} + \omega_0^2 e = -H\xi .$$ (24)

Thus, the overall system in error space can be described in standard state equation form

$$\dot{z} = Az + B\mu ,$$ (25)

where $$z = \begin{bmatrix} e & \dot{e} & \xi^T \end{bmatrix}^T ,$$ (26)

$$A = \begin{bmatrix} 0 & 1 & 0 \\ -\omega_0^2 & 0 & -H \\ 0 & 0 & F \end{bmatrix}, \quad B = \begin{bmatrix} 0 \\ 0 \\ G \end{bmatrix}.$$ (27)

Assume that $\{A, B\}$ is controllable. Therefore, there exists a control law,

$$\mu = -\begin{bmatrix} k_1 & k_2 & k_3 & k_4 \end{bmatrix}, \quad z = -Kz .$$ (28)

It is noted that if (28) stabilizes the closed-loop system, all states z become zero as time goes to infinity. In other words, the controller achieves perfect tracking. Substituting (28) into (25), the characteristic equation is given by

$$\Delta_c(s) = | sI - A_c | = s^4 + \left(\frac{R_f}{L_f} + \frac{k_3}{L_f} \right)s^3$$

$$+ \left\{ \frac{1}{C_f} \left(\frac{1}{L_f} + \frac{k_4}{L_f} \right) + \omega_o^2 \right\}s^2$$

$$+ \left[-\frac{k_2}{L_f C_f} + \omega_o^2 \left(\frac{R_f}{L_f} + \frac{k_3}{L_f} \right) \right]s$$

$$+ \left\{ -\frac{k_1}{L_f C_f} + \frac{\omega_o^2}{L_f C_f} + \frac{\omega_o^2 k_4}{L_f C_f} \right\}$$

$$= s^4 + a_3 s^3 + a_2 s^2 + a_1 s + a_0 .$$ (29)

3.1. Implementation of control law

To implement the control law (28), it needs to be expressed in terms of e and u. From (21), (22) and (28),

$$\mu = \ddot{u} + \omega_o^2 u = -k_1 e - k_2 \dot{e} - k_3 \xi_1 - k_4 \xi_2$$

$$= -k_1 e - k_2 \dot{e} - k_3 (\ddot{x}_1 + \omega_o^2 x_1) - k_4 (\ddot{x}_2 + \omega_o^2 x_2).$$ (30)

Furthermore, (24) can be concisely expressed by

$$\ddot{\eta} + \omega_o^2 \eta = -k_1 e - k_2 \dot{e} ,$$ (31)

where $$\eta := u + k_3 x_1 + k_4 x_2 .$$ (32)

If we define $\eta_1(s) = s^{-1}\left[-k_2 e(s) + \eta_1(s) \right]$ and $\eta_2(s) = \eta(s)$, we have

$$\begin{bmatrix} \dot{\eta}_1 \\ \dot{\eta}_2 \end{bmatrix} = \begin{bmatrix} 0 & -\omega_o^2 \\ 1 & 0 \end{bmatrix}\begin{bmatrix} \eta_1 \\ \eta_2 \end{bmatrix} + \begin{bmatrix} -k_1 \\ -k_2 \end{bmatrix}e ,$$ (33)

$$\eta = \begin{bmatrix} 0 & 1 \end{bmatrix}\begin{bmatrix} \eta_1 \\ \eta_2 \end{bmatrix}.$$ (34)

(33) and (34) are depicted by the box B in Fig. 5. From (32),

$$u = \eta - k_3 x_1 - k_4 x_2 = \eta - K_0 x ,$$ (35)

where $K_0 = \begin{bmatrix} k_3 & k_4 \end{bmatrix}$. Box A in Fig. 5 depicts (35).

3.2. Determination of controller gain K

Now, the remaining problem is to obtain the controller gain K that achieves the stability and the desired time response. As mentioned earlier, when one designs a digital controller by means of the emulation method, the transient response rate should be taken into account. Otherwise, the stability may be lost when the response speed is so fast that sufficient data cannot be gathered.

It may be possible to attempt to design a controller using the pole placement method on the overall characteristic equation, such as (29). Then the resulting continuous-time controller would be converted into a discrete-time one. If this procedure is pursued, what problem will arise? In fact, the most difficult problem of all is that there is no rule to select the proper pole locations so that the time response of the inner loop shall be not faster than a fixed sample period. It is also noted that the controller using the error space method guarantees robustly perfect tracking to a nondecaying reference input only if its characteristic equation (29) is stable. This implies that an ad-hoc method such as the two-time scale is not necessary when K is designed. In this paper, the design procedure is divided into two steps. First, K_0 is determined such that the time response of the inner loop has the settling time of 15~20 times the sampling period. This step is performed by the CRA. Secondly, after K_0 is

obtained, we try to find a $\begin{bmatrix} k_1 & k_2 \end{bmatrix}$ so that the overall system with the given K_0 is stable and has a good transient response. The second step is also carried out using the CRA.

Let's go to the first step. From (4) and (5), the UPS plant is

$$\dot{x} = Fx + Gu + G_1 w,$$
$$y = Hx,$$
(36)

and the control input is

$$u = \eta_2 - k_3 x_1 - k_4 x_2$$
$$= \eta_2 + u_2,$$
(37)

where $u_2 = -k_3 x_1 - k_4 x_2$. Combining (36) and (37), we get

$$\dot{x} = Fx + G(\eta_2 + u_2) + G_1 w$$
$$= Fx + Gu_2 + G\eta_2 + G_1 w$$
$$= [F - GK_o]x + G\eta_2 + G_1 w,$$
$$y = Hx.$$
(38)

With $w = 0$, the transfer function of (38) is given by

$$G_{pc} = \frac{y(s)}{\eta_2(s)} = \frac{\dfrac{1}{L_f C_f}}{s^2 + (\dfrac{R_f}{L_f} + \dfrac{k_3}{L_f})s + \dfrac{k_4 + 1}{L_f C_f}}.$$
(39)

Next we set the target polynomial for the inner loop to

$$\Delta_i^*(s) = s^2 + \delta_{i1} s + \delta_{i0}.$$
(40)

If we select the proper target polynomial, it is obvious that K_0 will be obtained uniquely. That is, we have

$$k_3 = L_f \delta_{i1} - R_f,$$
(41)

$$k_4 = L_f C_f \delta_{i0} - 1.$$
(42)

Since (39) is merely of order 2, the target polynomial (40) can be easily determined by the pole placement method. Here in order to propose a unified approach the CRA is employed. Then (40) can be easily found by choosing α_1 and τ, which are defined in section 2.2:

$$\delta_{i1} = \frac{\alpha_1}{\tau}, \quad \delta_{i0} = \frac{\delta_{i1}}{\tau}.$$
(43)

In particular, since the settling time can be exactly controlled by the value of τ while α_i is fixed, the response rate is easily dealt with. The characteristic ratios, α_i s are closely related to the damping and the stability. The details related to the selection of α_i

and τ are referred to [4,5,7].

Next, we will find $\begin{bmatrix} k_1 & k_2 \end{bmatrix}$. This gain will also be determined by the CRA. Similar to the previous step, we choose a fourth-order target polynomial

$$\Delta_c^*(s) = s^4 + \delta_3 s^3 + \delta_2 s^2 + \delta_1 s + \delta_0 s.$$
(44)

However, we see from (29) that where $\begin{bmatrix} k_3 & k_4 \end{bmatrix}$ is given, the characteristic polynomial coefficients a_2 and a_3 are already known. Thus, we cannot assign all α_i s and τ independently. For this case, we suggest a guide of selecting α_1, α_2 and τ as follows:

(i) δ_3 and δ_2 should be the same as a_3 and a_2, respectively. Therefore, α_3 is given a priori.

(ii) Select α_2 approximately larger than 2. Then calculate δ_1 using δ_3, δ_2 and α_2:

$$\delta_1 = \frac{\delta_2^2}{\delta_3 \alpha_2}.$$

(iii) We take no account of τ but select an $\alpha_1 > 2.5$. Calculate δ_0 using only α_1 as follows:

$$\delta_0 = \frac{\delta_1^2}{\delta_2 \alpha_1}.$$

By comparing (29) with (44), $\begin{bmatrix} k_1 & k_2 \end{bmatrix}$ is determined. If the resulting performance is unsatisfactory, then change α_2 and α_1 and repeat the above procedure.

3.3. Digitization of continuous-time controller

Finally, in order to obtain the digital controller, we apply a discretization method such as the Tustin approximation to the continuous-time controller. A discrete state space representation of (33) and (34) can be written as follows:

$$\bar{\eta}(k+1) = A_D \bar{\eta}(k) + B_D e(k),$$
(45)

$$\eta(k) = C_D \bar{\eta}(k) + D_D e(k),$$
(46)

where $\bar{\eta}(k) = \begin{bmatrix} \eta_1(k) & \eta_2(k) \end{bmatrix}^T$. If we let the sample variables of $x_1(t)$ and $x_2(t)$ be $x_1(k)$ and $x_2(k)$, respectively, the discrete time controller corresponding to (35) becomes

$$u(k) = \eta(k) - k_3 x_1(k) - k_4 x_2(k).$$
(47)

Remark 1: The digital control output $u(k)$ in (47) depends on the input at the same time point. It may be desirable to derive a digital control law that would

only require inputs from the previous time. It is unusual for such a control law to be considered in the state space method. However, if we design a digital controller in compensator form, the time delay due to ZOH and computation can be associated with the input actuator. An example for this case will be shown in Section 4.

4. SIMULATION RESULTS

To evaluate the performance of the proposed controller, simulations are carried out using Simulink®. The system parameters considered for the simulations are given in Table 2.

Table 2. System parameters.

System parameters		Values
Filter	Filter inductance (L_f)	$200\,[\mu H]$
	Filter resistance (R_f)	$0.08\,[\Omega]$
	Filter capacitance (C_f)	$120\,[\mu F]$
Input voltage $(v_c^*(t))$		$\pm150\,[V]$
DC-link (v_{dc})		$270\,[V]$
IGBT's switching frequency (f_{switch})		$8\,[kHz]$
Sampling frequency (f_s)		$8\,[kHz]$

When K_0 is determined, we have selected $\alpha_1 = 2.6$ and $\tau = 0.41667\,m\sec$. Following the steps in section 3.2, the control gains of inner loop were determined to be

$$[k_3 \quad k_4] = [1.1680 \quad -0.6406].$$

By choosing $[\alpha_1 \quad \alpha_2] = [2.5 \quad 2]$, we obtain

$$[k_1 \quad k_2] = [-1.61900 \quad -418.2497].$$

Converting (33) and (34) using Tustin's method into (45) and (46), we have

$$A_D = \begin{bmatrix} 0.99889028557976 & -17.75543072386747 \\ 0.00012493064285 & 0.99889028557976 \end{bmatrix}$$

$$B_D = \begin{bmatrix} 158093.334662581 \\ 428.130485686 \end{bmatrix},$$

$$C_D = [0.0000000078081 \quad 0.0001249306428],$$

$$D_D = [0.02675815535535].$$

The digital controller designed has been examined by using Simulink®. The most important requirements for a high performance UPS are the THD less than 5% and a fast response with little overshoot over all kinds of loading conditions. For the sake of the performance evaluations, we have considered three load conditions: no load, a resistive load of 10kW, and a nonlinear rectifier load of 10kW. In each case, the THD was
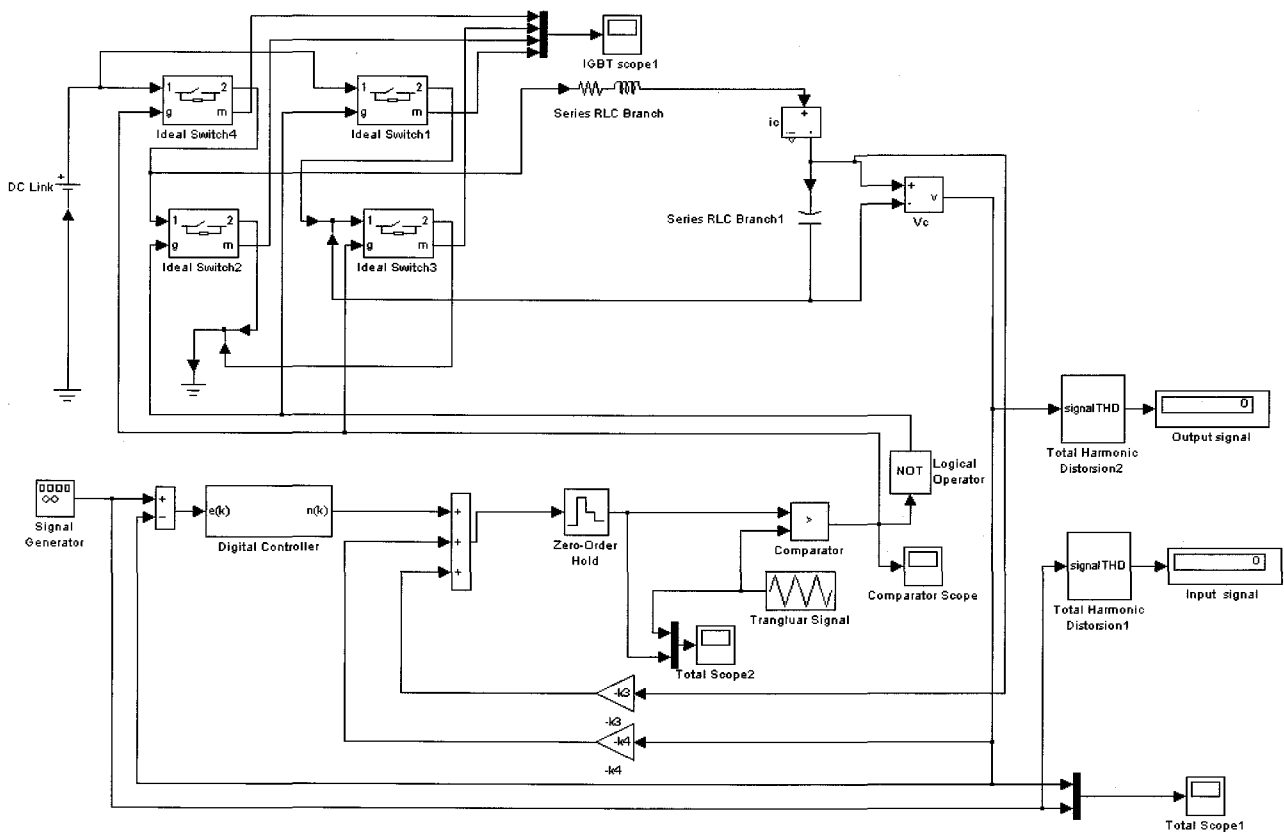

Fig. 7. UPS inverter system with the proposed controller.

evaluated. Fig. 7 shows the UPS inverter system with the proposed controller, where the parameters of IGBT used are as follows:

Initial state: open, $R_{snubber} = 0.1[\Omega]$,

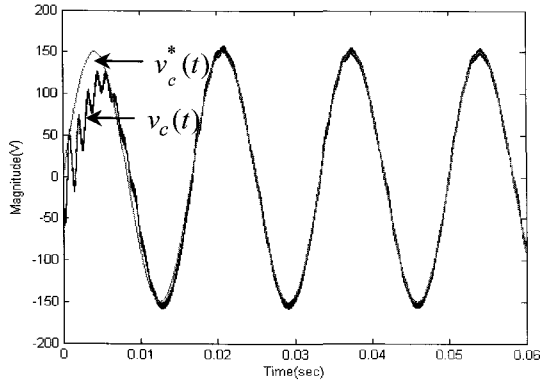$R_{on} = 0.01[\Omega]$, $C_{snubber} = 0.22[\mu F]$.

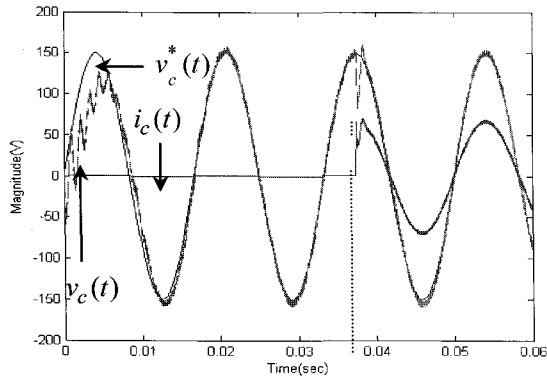Fig. 8. Output response under no load.

Fig. 9. Output response under a linear load change.

Fig. 8 shows the output response of the UPS system under no load condition. It is seen that the proposed controller tracks the reference signal with very low tracking error. The THD of the response was about 3.99%.

Fig. 9 shows the output response for the case of a 10kW resistive load that is abruptly applied at the peak phase (around $t = 0.037$ sec). This is to examine how large the overshoot occurs at the extreme condition and how fast the controller responds. We see from Fig. 9 that the maximum overshoot was about 50% and the step change has been settled down within half a period. In this case, the THD shows about 4.13%.

For the third load condition, we have considered a rectifier load which has nonlinear characteristics. Fig. 10 shows the block of the rectifier load constructed for the simulation. The rectifier parameters are as follows:

$R_{Lon} = 0.22784[\Omega]$, $R_{diode} = 0.01[\Omega]$,

$L_{load} = 1[\mu H]$, $R_{diode} = 10[\Omega]$, $C_{load} = 50420[\mu F]$,

$C_{diode} = 0.01[\mu F]$, $R_{load} = 10.9[\Omega]$.

As shown in Fig. 11, the current characteristics have a very high crest factor signifying highly nonlinear load. In Fig. 12, the output response and reference voltage are shown. The rectifier load was abruptly applied at the peak phase of reference voltage (around $t = 0.037$ sec). As a result, the tracking performance seems to be acceptable but the THD, which was about 12.04%, does not meet the specifications. In conclusion, it has been shown that in all the cases the proposed controller has satisfactory tracking and time response performances.
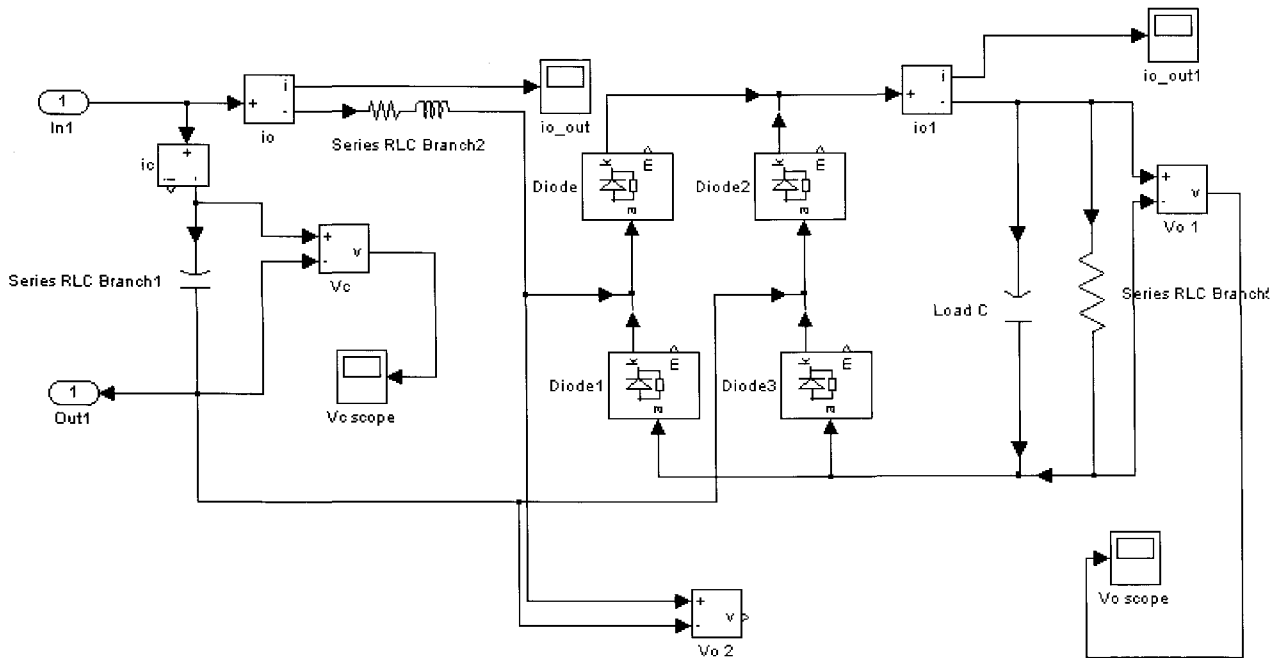

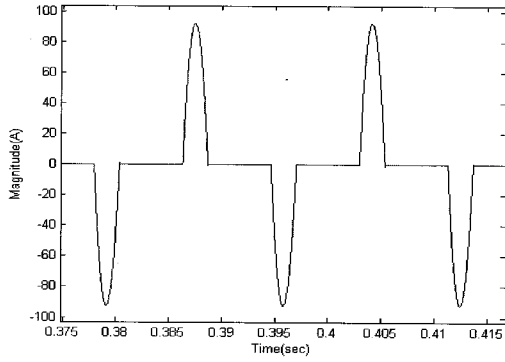Fig. 10. Nonlinear rectifier load.
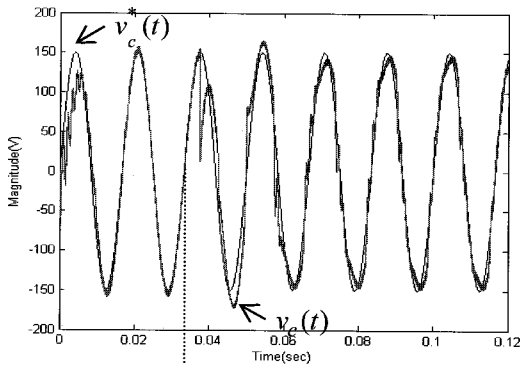
Fig. 11. Current waveform of rectifier load.

Fig. 12. Output response under a nonlinear load change.

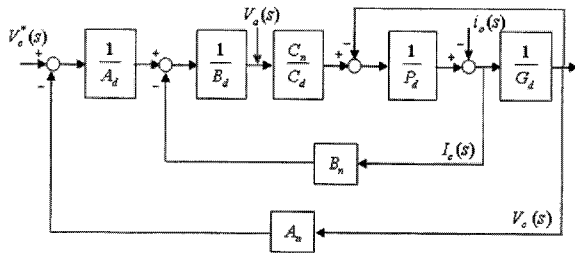Fig. 13. Block diagram of UPS system with PI and.

In addition, to compare the performance of the proposed controller with the conventional method, another example performed on a cascade control structure is given. Fig. 13 shows its block diagram in which PI and first-order controllers are occupied. In particular, a rational transfer function C_n/C_d is inserted in front of the plant to compensate the time delay T_d that arises from the zero order hold (ZOH) (which is about $T_s/2$) and the delayed computer output of the controller by one sample time T_s.

PI controller: $\dfrac{A_n}{A_d} = \dfrac{b_1 s + b_0}{s}$,

First-order controller: $\dfrac{B_n}{B_d} = \dfrac{a_1 s + a_0}{s + a_2}$,

L-C filter: $\dfrac{1}{P_d} = \dfrac{1}{L_f s + R_f}$, $\dfrac{1}{G_d} = \dfrac{1}{C_f s}$,

Pade approximation of time delay due to ZOH and

computation: $\dfrac{C_n}{C_d} = \dfrac{1 - T_d s/2}{1 + T_d s/2}$, $(T_d = T_s/2 + T_s)$.

Herein, the values of plant parameters are the same as those in Table 2. The transfer function of the closed-loop system is given by

$$\frac{V_c^*(s)}{V_c(s)} = \frac{n(s)}{p(s)}, \tag{48}$$

where

$$n(s) = C_n, \tag{49}$$

$$p(s) = G_d P_d B_d C_d A_d + G_d A_d C_n B_n + C_n A_n + B_d C_d A_d$$

$$= \frac{3C_f L_f T_s}{4} s^5 + \left(-\frac{3C_f T_s a_1}{4} + \frac{3C_f L_f a_2 T_s}{4} + \frac{3C_f R_f T_s}{4} + C_f L_f\right) s^4$$

$$+ \left(C_f a_1 - \frac{3C_f T_s a_0}{4} + \frac{3T_s}{4} + C_f R_f + \frac{3C_f R_f a_2 T_s}{4} + C_f L_f a_2\right) s^3$$

$$+ \left(C_f R_f a_2 + 1 + \frac{3T_s a_2}{4} + C_f a_0 - \frac{3T_s b_1}{4}\right) s^2 + \left(b_1 - \frac{3T_s b_0}{4} + a_2\right) s + b_0.$$

Next, we set the target polynomial of the overall system. In Section 2.2, it is shown that the polynomial can be generated by using (9) and (10) with holding conditions of (11) and (12). Here, by selecting $a_0 = 2.31*10^7$, $\alpha_1 = 2.8$ and $\tau = 1$ [ms], we have the target polynomial

$$p^*(s) = 2.25*10^{-12} s^5 + 9.05*10^{-8} s^4$$

$$+ 1.3*10^{-3} s^3 + 8.25 s^2 \tag{50}$$

$$+ 2.31 \times 10^4 s + 2.31 \times 10^7.$$

Then the gains of continuous-time controller have been determined from the algebraic relation between $p(s)$ and $p^*(s)$ as follows:

$$[a_2 \; a_1 \; a_0 \; b_1 \; b_0] = [4.15 \times 10^4 \; 2.47 \; 1.19 \times 10^4$$

$$- 1.63 \times 10^4 \; 2.31 \times 10^7].$$

Applying digitization by the Tustin approximation to the designed continuous-time controller, the digital controller is given by

$$C_1(z) = \frac{0.9z + 0.48}{z + 0.44}, \tag{51}$$

$$C_2(z) = \frac{-0.26z^2 + 0.05z + 0.31}{z^2 - 0.56z - 0.44}. \tag{52}$$

Fig. 14 shows the digital controllers implemented by means of the Simulink®. Also, Fig. 15 presents the output response under a linear load change. The THD of the response was about 4.47%. It is also shown that the PI and first-order controllers have a fast transient response and relatively small overshoot over a linear
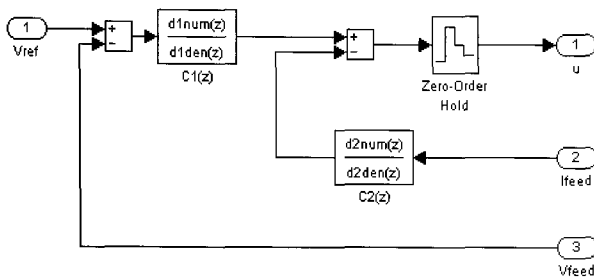
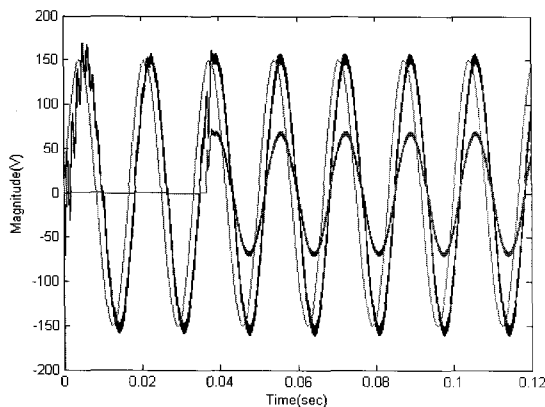Fig. 14. Digital PI and First-order controllers.

Fig. 15. Output response under a linear load change.

load change. On the contrary it cannot evade the phase delay and steady-state error due to the type of the reference input $v^*(t)$. To eliminate those effects, a compensator like notch-filter or IMC controller may be used in the outer-loop additionally.

Thus, we can conclude that the error-space approach is preferable to the conventional method in the sense that the former has an ability to robustly track the reference signal with a relatively lower-order controller.

5. CONCLUSIONS

For the design of a digital controller for a UPS inverter that should have robust AC-voltage tracking ability, a design method based on the error-state approach and the characteristic ratio assignment has been proposed. The error state approach ensures asymptotically perfect tracking only if the closed-loop system remains stable. It turns out that the proposed controller allows exact sine-wave tracking even though the plant parameters have some uncertainty and even when one changes the linear load abruptly. When we design a digital controller by means of the emulation method with a fixed sampling time, we are faced with the problem that the speed of the time response must be limited.

As a possible method to the problem, the characteristic ratio assignment was introduced. When we deal with the step response requirements such as

overshoot and settling time, the CRA is applied much easier compared with the pole-placement method. Through several real-time simulations using Simulink®, it has been verified that the proposed controller satisfies the tracking performance very well over all linear load conditions. For a nonlinear load condition such as a rectifier, the tracking performance seems to be acceptable, but its THD (12.04%) does not meet the given specification.

REFERENCES

[1]   M. J. Yazdanpanah, E. Semsar, and B. Siahkolah, "An H_∞ robust controller for single phase PWM inverters," *Proc. of the 15th IFAC WORLD Congress*, Barcelona, Spain, 2002.

[2]   M. J. Ryan and R. D. Lorenz, "A high performance sine wave inverter controller with capacitor current feedback and 'back-EMF' decoupling," *Proc. of IEEE PESC con. Rec.*, pp. 507-513, 1995.

[3]   A. Kawamura and T. Yokoyama, "Comparison of five different approaches for real time digital feedback control of PWM inverter," *Proc. of IEEE Ind. Appl. Society Conf.* vol. 2, pp. 1000-1005, 1990.

[4]   Y. C. Kim, L. H. Keel, and S. P. Bhattacharyya, "Transient response control via characteristic ratio assignment," *IEEE Trans. on Automatic Control*, vol. AC-48, no. 12, pp.2238-2244, DEC. 2003.

[5]   K. S. Kim, Y. C. Kim, L. H. Keel, and S. P. Bhattacharyya, "PID controller design with time response specifications," *Proc. of the 2003 American Cont. Conf.*, Denver, pp. 5005-5010, 2003.

[6]   G. F. Franklin, J. D. Powel, and A. Emani-Naeini. *Feedback Control of Dynamic Systems*, Prentice-Hall, Upper Saddle River, New Jersey, 2002.

[7]   S. Manabe, "Coefficient diagram method," *Proc. of the 14th IFAC Symposium on Automatic Control in Aerospace*, Seoul, Korea, pp. 199-210 1998.

[8]   C. Kessler, "Ein Beitrag zur Theorie mehrschleifiger Regelungen," *Regelung-stechnik* vol. 8, no. 8, pp. 261-266, 1960.
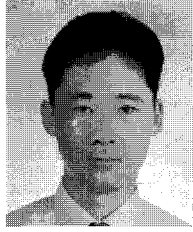
Young-Tae Woo was born on Oct. 4, 1971. He received the B.S. and M.S. degrees in Electronic Engineering from Chungbuk National University, Cheong-u, Korea in 1997, and 1999, respectively. He is currently working toward his Ph.D. degree. His research interests include robust control, system identification and digital control.
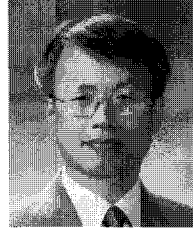
Young-Chol Kim received the B.S. degree in Electrical Engineering from Korea University, Korea in 1981, and the M.S. and Ph.D. degrees in Electrical Engineering from Seoul University, Korea in 1983 and 1987 respectively. Since March 1988, he has been with the School of Electrical & Computer Engineering, Chungbuk National University, Korea, where he is currently a Professor. He was a Post-doctoral Fellow at Texas A&M University, 1992-1993, and a Visiting Research Fellow at the COE-ISM, Tennessee State Univ. / Vanderbilt Univ., 2001-2002. He served as an Associate Editor for the Korean Institute of Electrical Engineers, 1996-1998. He has been the Director of the Technical Society of Control and Instrument, KIEE since 2004. His research interests include robust control in parameter space and low-order controller design based on the Characteristic Ratio Assignment.